49th AIAA/ASME/ASCE/AHS/ASC Structures, Structural Dynamics, and Materials Conference
 16t
7 - 10 April 2008, Schaumburg, IL

AIAA 2008-1878

A comprehensive FE model for the analysis of Multilayered Structures Subjected to Multifiled Loadings

E. Carrera* and P. Nali†

Department of Aeronautics and Aerospace Engineering, Politecnico di Torino, Italy

A. Calvi‡

ESTEC, European Space Agency, Noordwijk, The Netherlands

This work deals with classical variational statements for the analysis of layered structures under the effect of four different fields: mechanical, thermal, electrical and magnetic. Constitutive equations, in terms of coupled mechanical-thermal-electrical-magnetic field variables, are obtained on the basis of a thermodynamic approach. The Principle of Virtual Displacements (PVD) is employed. A number of particular cases of the considered variational statement is proposed. A new condensed notation is introduced into the Carrera's Unified Formulation (CUF) framework, which leads to governing equations and Finite Element (FE) matrices in terms of a few fundamental nuclei. The FE case for multilayerd plates is addressed to. Numerical results consist in a critical comparison between several exact solutions found in literature and the corresponding results obtained by MUL2 FEM code, which has been developed coherently with the presented formulation.

Nomenclature

A = the surface involved by loading;
B_i = magnetic inductance component;
C = specific heat per unit mass;
C_{ijkl} = elastic coefficients - Hooke's law;
$\boldsymbol{D}$ = differential operator;
D_i = electrical displacement component;
d_{nm} = electromagnetic coefficients;
E_i = electric field component;
e_{ijn} = piezoelectric coefficients;
$F_\tau(z)$ = set of polynomials independent functions;
G = Gibbs free energy per unit of volume;
$\boldsymbol{H}$ = constitutive matrix;
H_i = magnetic field component;
h_k = k-layer thickness;
$k^{k\tau sij}$ = fundamental nucleus;
L_e = work made by external loads;
N = order of expansion;
N_i = i^{th} shape function;
N_l = number of layers;

*Professor, Aerospace Department, Politecnico di Torino, Corso Duca degli Abruzzi, 24, 10129 Torino, Italy, erasmo.carrera@polito.it.

†PhD Student, Aerospace Department, Politecnico di Torino, Corso Duca degli Abruzzi, 24, 10129 Torino, Italy, pietro.nali@polito.it.

‡Senior Scientist, ESA/ESTEC, P.O. Box 299, Noordwijk, 2200 AG, The Netherlands, adriano.calvi@esa.int.

N_n = number nodes of the considered finite element;
$\boldsymbol{P}$ = vector of nodal external loads;
p_n = pyroelectric coefficients;
q_{ijn} = piezomagnetic coefficients;
$\boldsymbol{Q}$ = vector of nodal unknowns;
r_n = pyromagnetic coefficients;
$\boldsymbol{\mathcal{S}}$ = vector of extensive variables;
U = internal energy per unit of volume;
$\boldsymbol{U}^k$ = vector of primary unknowns;
V = volume;

δ = the variational symbol;
δT = increment of temperature;
ϵ_{ij} = strains tensor;
ε_{ij} = permittivity coefficients;
$\boldsymbol{\mathcal{E}}$ = vector of intensive variables;
η = variation of entropy per unit of volume;
θ = temperature variation;
θ_{ref} = temperature of reference;
λ_{ij} = stress-temperature coefficients;
μ_{ij} = magnetic permeability coefficients;
ρ = density;
σ_{ij} = stress tensor;
ϕ = electric potential;
ψ = magnetic potential;
Ω_k = layer middle surface;

CUF : Carrera's Unified Formulation;
$CUFMM$: Carrera's Unified Formulation Mixed Methods;
$ESLM$: Equivalent Single Layer Model;
FE : Finite Element;
FEM : Finite Element Method;
LWM : Layer Wise Model;
MFP : MultiField Problem;
MLS : MultiLayered Structure;
PVD : Principle of Virtual Displacements;
$RMVT$: Reissner's Mixed Variational Theorem;
TPS : Thermal Protection System.

I. Introduction

Conventional and unconventional spacecraft constructions have constantly been characterized by an extensive use of MultiLayered Structures (MLSs). First, layers of metallic/ceramic materials have been adopted as Thermal Protection Systems (TPS). Recently, advanced composite materials have been used to build large parts of spacecrafts. Metallic and composite structures can be considered as *conventional* multilayered application; these are, in fact, largely applied in space technology. Moreover, other *unconventional* MLSs are under consideration for their possible use for the next generation of spacecrafts: smart structures (in which piezoelectric layers or patches are embedded in the structure) and inflatable structures (made by many layers of very different materials, including TPS). Accurate structural modelling of multilayered made structures when subjected to various fields (mechanical, thermal, electrical) is a crucial point for the structural analyst. The possibility of building a real time control for smart structures for the practical space structures is still to be demonstrated. Available commercial software, which has not been designed for the analysis of the structures above mentioned, can experience some difficulties in their simulation. On the other hand a validation of advanced and more reliable computational models, which applications were restricted to *academic* problems, is mandatory whenever a real construction is made and a testing campaign is scheduled.

There are many open problems concerning the mechanical modelling of these structures. Theories and computational models implemented in available codes have been, in fact, mostly devoted to simulation of traditional one-layered structures. Amendments to these findings are mandatory to capture the effective mechanical, thermal and electrical fields in each layer.
A number of requirements must be taken into account for an accurate analysis of MultiField Problems (MFPs) and MLSs. The following points deal with in this paper:

1. The Constitutive equations must be derived in a consistent form.
2. The Coupling among the various fields should be accurately described.
3. Inter-layer continuity of the relevant variables must be guaranteed.
4. The employed kinematic model must be rich enough to describe the localized through-the-thickness-distribution of the involved variables in the various layers.

Reference to a thermodynamic basis is mandatory for point 1.[1]
For the fulfillment of point 2, the constitutive relations are coupled. For the general case, thermo-electro-magnetic-mechanical coupling can be included in the formulation.[2] As far as point 3 is concerned, it should be pointed out that a classical choice of primary variables for the various fields could violate some interlaminar continuities. This is the case of transverse shear and normal stresses, which for equilibrium reasons, must be continuous at each layer interface. Such continuity is not enforced in classical modeling which only makes use of displacement variables.[3] The same could be said for transverse electrical displacements or transverse magnetic inductance.[4,5]
Concerning point 4, it is well known that the use of variable kinematic models is mandatory in MLSs subjected to MFP loadings. These loadings, in fact, have an *isotropic/anisotropic* and *localized* nature. For instance, the thermal field, being scalar, is isotropic by definition while the electrical and magnetic fields, being vectorial, can be isotropic or anisotropic. Loadings from these fields are completely different from those from mechanical cases. Consequently, kinematic models that were originally proposed for plate and shell structures subjected to mechanical loading could undergo difficulties analyzing MFPs. Modelings that permits the use of both Equivalent Single Layer Models (ESLM) and Layer Wise Models (LWM), are mandatory in these cases.
Recent research works carried out at Politecnico di Torino, by Carrera's Unified Formulation (CUF) and Mixed Methods (CUFMM) for plate and shell analyses, have established a hierarchic finite element formulation for MLSs subjected to multifield loading (e.g. mechanical-thermal-electrical-magnetic).[2,4,5] This approach consists in a valuable tool for the analysis of both conventional and unconventional structures.
Starting from the last work,[2] this paper consists in a PVD (Principle of Virtual Displacement) investigation for multilayered plates with mechanic, thermal, electrical and magnetic coupling.

II. Constitutive equations for multifield problems

The constitutive equations are derived, in this section, in the linear case for the considered MFPs. Standard tensor notation is used and Einstein's summation convention is implied over repeated indices. A set of intensive variables θ, ϵ, E and H, which are respectively the increment in temperature, strain, electric field and magnetic field, are first assumed as independent variables. The relevant thermodynamic function is the Gibbs free energy per unit of volume G[1,6,7] which is here extended to include the magnetic field:

$$G = U + \sigma_{ij}\epsilon_{ij} - \theta\eta - E_i D_i - H_i B_i, \tag{1}$$

where:
U = internal energy per unit of volume (function of η, ϵ_{ij}, D_i and B_i);
η = variation of entropy per unit of volume;
σ_{ij} = stress tensor;
D_i = electrical displacements vector;
B_i = magnetic inductancesf vector.

Gibbs free energy can be written as a quadratic form in accord with Ikeda:[1]

$$\begin{aligned} G = \frac{1}{2}\Bigg(& \theta^2 \frac{\partial^2 G}{\partial \theta^2} + \epsilon_{ij}\epsilon_{lm}\frac{\partial^2 G}{\partial \epsilon_{ij}\partial \epsilon_{lm}} + E_i E_l \frac{\partial^2 G}{\partial E_i \partial E_l} + H_i H_l \frac{\partial^2 G}{\partial H_i \partial H_l} + \theta \epsilon_{lm}\frac{\partial^2 G}{\partial \theta \partial \epsilon_{lm}} + \\ & + \theta E_l \frac{\partial^2 G}{\partial \theta \partial E_l} + \theta H_l \frac{\partial^2 G}{\partial \theta \partial H_l} + \epsilon_{ij}\theta \frac{\partial^2 G}{\partial \epsilon_{ij}\partial \theta} + \epsilon_{ij} E_l \frac{\partial^2 G}{\partial \epsilon_{ij}\partial E_l} + \epsilon_{ij} H_l \frac{\partial^2 G}{\partial \epsilon_{ij}\partial H_l} + \\ & + E_i \theta \frac{\partial^2 G}{\partial E_i \partial \theta} + E_i \epsilon_{lm}\frac{\partial^2 G}{\partial E_i \partial \epsilon_{lm}} + E_i H_l \frac{\partial^2 G}{\partial E_i \partial H_l} + H_i \theta \frac{\partial^2 G}{\partial H_i \partial \theta} + H_i \epsilon_{lm}\frac{\partial^2 G}{\partial H_i \partial \epsilon_{lm}} + \\ & + H_i E_l \frac{\partial^2 G}{\partial H_i \partial E_l}\Bigg). \end{aligned} \tag{2}$$

The exact differential of G is:

$$dG = \sigma_{ij} d\epsilon_{ij} - \eta d\theta - D_i dE_i - B_i dH_i, \tag{3}$$

where:

$$\sigma_{ij} = \left[\frac{\partial G}{\partial \epsilon_{ij}}\right]_{\theta,E,H}, \quad \eta = -\left[\frac{\partial G}{\partial \theta}\right]_{\epsilon,E,H}, \quad D_i = -\left[\frac{\partial G}{\partial E_i}\right]_{\theta,\epsilon,H}, \quad B_i = -\left[\frac{\partial G}{\partial H_i}\right]_{\theta,\epsilon,E}. \tag{4}$$

Subscripts refer to the quantities to be kept constant in the differentiation.
Substituting Eq.(2) into Eq.(4) one has:

$$\eta = \theta\left[-\frac{\partial^2 G}{\partial \theta^2}\right]_{\epsilon,E,H} + \epsilon_{ij}\left[-\frac{\partial^2 G}{\partial \theta \partial \epsilon_{ij}}\right]_{E,H} + E_i\left[-\frac{\partial^2 G}{\partial \theta \partial E_i}\right]_{\epsilon,H} + H_i\left[-\frac{\partial^2 G}{\partial \theta \partial H_i}\right]_{\epsilon,E}; \tag{5}$$

$$\sigma_{ij} = \theta\left[\frac{\partial^2 G}{\partial \epsilon_{ij}\partial \theta}\right]_{E,H} + \epsilon_{ij}\left[\frac{\partial^2 G}{\partial \epsilon_{ij}\partial \epsilon_{lm}}\right]_{\theta,E,H} + E_l\left[\frac{\partial^2 G}{\partial \epsilon_{ij}\partial E_l}\right]_{\theta,H} + H_l\left[\frac{\partial^2 G}{\partial \epsilon_{ij}\partial H_l}\right]_{\theta,E}; \tag{6}$$

$$D_i = \theta\left[-\frac{\partial^2 G}{\partial E_i \partial \theta}\right]_{\epsilon,H} + \epsilon_{ij}\left[-\frac{\partial^2 G}{\partial E_l \partial \epsilon_{ij}}\right]_{\theta,H} + E_i\left[-\frac{\partial^2 G}{\partial E_i \partial E_j}\right]_{\theta,\epsilon,H} + H_i\left[-\frac{\partial^2 G}{\partial E_i \partial H_j}\right]_{\theta,\epsilon}; \tag{7}$$

$$B_i = \theta\left[-\frac{\partial^2 G}{\partial H_i \partial \theta}\right]_{\epsilon,E} + \epsilon_{ij}\left[-\frac{\partial^2 G}{\partial H_l \partial \epsilon_{ij}}\right]_{\theta,E} + E_i\left[-\frac{\partial^2 G}{\partial H_i \partial E_j}\right]_{\theta,\epsilon} + H_i\left[-\frac{\partial^2 G}{\partial H_i \partial H_j}\right]_{\theta,\epsilon,E}. \tag{8}$$

The following coefficients can be defined:

$$\begin{aligned} & \frac{\rho C^{\epsilon,E,H}}{\theta_{ref}} = -\left[\frac{\partial^2 G}{\partial \theta^2}\right]_{\epsilon,E,H} = \left[\frac{\partial \eta}{\partial \theta}\right]_{\epsilon,E,H}, && C_{ijlm}^{\theta,E,H} = \left[\frac{\partial^2 G}{\partial \epsilon_{ij}\partial \epsilon_{lm}}\right]_{\theta,E,H} = \left[\frac{\partial \sigma_{ij}}{\partial \epsilon_{lm}}\right]_{\theta,E,H}, \\ & \varepsilon_{ij}^{\theta,\epsilon,H} = -\left[\frac{\partial^2 G}{\partial E_i \partial E_j}\right]_{\theta,\epsilon,H} = \left[\frac{\partial D_i}{\partial E_j}\right]_{\theta,\epsilon,H}, && \mu_{ij}^{\theta,\epsilon,E} = -\left[\frac{\partial^2 G}{\partial H_i \partial H_j}\right]_{\theta,\epsilon,E} = \left[\frac{\partial B_i}{\partial H_j}\right]_{\theta,\epsilon,E}, \\ & \lambda_{ij}^{E,H} = -\left[\frac{\partial^2 G}{\partial \theta \partial \epsilon_{ij}}\right]_{E,H} = -\left[\frac{\partial \sigma_{ij}}{\partial \theta}\right]_{\epsilon,E,H} = \left[\frac{\partial \eta}{\partial \epsilon_{ij}}\right]_{\theta,E,H}, && p_i^{\epsilon,H} = -\left[\frac{\partial^2 G}{\partial \theta \partial E_i}\right]_{\epsilon,H} = \left[\frac{\partial D_i}{\partial \theta}\right]_{\epsilon,E,H} = \left[\frac{\partial \eta}{\partial E_i}\right]_{\theta,\epsilon,H}, \\ & e_{lij}^{\theta,H} = -\left[\frac{\partial^2 G}{\partial \epsilon_{ij}\partial E_l}\right]_{\theta,H} = -\left[\frac{\partial \sigma_{ij}}{\partial E_l}\right]_{\theta,\epsilon,H} = \left[\frac{\partial D_l}{\partial \epsilon_{ij}}\right]_{\theta,E,H}, && r_i^{\epsilon,E} = -\left[\frac{\partial^2 G}{\partial \theta \partial H_i}\right]_{\epsilon,E} = \left[\frac{\partial \eta}{\partial H_i}\right]_{\theta,\epsilon,E} = \left[\frac{\partial B_i}{\partial \theta}\right]_{\epsilon,E,H}, \\ & q_{lij}^{\theta,E} = -\left[\frac{\partial^2 G}{\partial \epsilon_{ij}\partial H_l}\right]_{\theta,E} = -\left[\frac{\partial \sigma_{ij}}{\partial H_l}\right]_{\theta,\epsilon,E} = \left[\frac{\partial B_l}{\partial \epsilon_{ij}}\right]_{\theta,E,H}, && d_{ij}^{\theta,\epsilon} = -\left[\frac{\partial^2 G}{\partial E_i \partial H_j}\right]_{\theta,\epsilon} = \left[\frac{\partial D_i}{\partial H_j}\right]_{\theta,\epsilon,E} = \left[\frac{\partial B_i}{\partial E_j}\right]_{\theta,\epsilon,H}, \end{aligned} \tag{9}$$

with:

ρ = density;	$C^{\epsilon,E,H}$ = specific heat per unit mass;
θ_{ref} = temperature of reference ;	C_{ijlm} = elastic coefficients - Hooke's law;
ε_{ij} = permittivity coefficients;	μ_{ij} = magnetic permeability coefficients;
λ_{ij} = stress-temperature coefficients;	p_i = pyroelectric coefficients;
e_{lij} = piezoelectric coefficients;	r_i = pyromagnetic coefficients;
q_{lij} = piezomagnetic coefficients;	d_i = magneto-electric coupling coefficients.

The first four constants in Eqs.(9) are principal constants in the respective individual systems; the latter six are coupling constants between two of the four considered fields. Upon introducing the constants of Eqs.(9), the following constitutive equations in the coupled four-field system are obtained by Eqs.(5)-(8):

$$\begin{aligned} \eta &= \frac{\rho}{\theta_{ref}} C^{\epsilon,E,H}\theta + \lambda_{ij}^{E,H}\epsilon_{ij} + p_i^{\epsilon,H}E_i + r_i^{\epsilon,E}H_i, & \sigma_{ij} &= -\lambda_{ij}^{E,H}\theta + C_{ijlm}^{\theta,E,H}\epsilon_{lm} - e_{ijl}^{\theta,H}E_l - q_{ijl}^{\theta,E}H_l, \\ D_l &= p_l^{\epsilon,H}\theta + e_{lij}^{\theta,H}\epsilon_{ij} + \varepsilon_{lm}^{\theta,\epsilon,H}E_m + d_{lm}^{\theta,\epsilon}H_m, & B_l &= r_l^{\epsilon,E}\theta + q_{lij}^{\theta,E}\epsilon_{ij} + d_{lm}^{\theta,\epsilon}E_m + \mu_{lm}^{\theta,\epsilon,E}H_m. \end{aligned} \tag{10}$$

As emphasized by Ikeda,[1] physical constants are introduced by second derivative of the relevant thermodynamic function. Each coupling constant is a second derivative with respect to two different variables, and is therefore considered to have a different meaning when interchanging the order of differentiation. For instance, from the definition given above, two kind of piezoelectric constant,

$$e_{lij}^{\theta,H} = \left[\frac{\partial D_l}{\partial \epsilon_{ij}}\right]_{\theta,E,H} \quad \text{and} \quad \widetilde{e}_{lij}^{\theta,H} = -\left[\frac{\partial \sigma_{ij}}{\partial E_l}\right]_{\theta,\epsilon,H},$$

are derived. The former e represents the electric flux density versus unit strain, whereas the latter $\widetilde{e}$ represents stress versus unit electric field. It turns out that these correspond to the direct and converse piezoelectric effect, respectively. The piezoelectric coupling term in the third of Eqs.(10) indicates the direct effect; that in the second of Eqs.(10) represents the converse effect. The equality of direct and converse effect is thus self-evident. Similar facts are found for the other coupling constants (λ_{ij}, p_i, r_i, q_{lij}, and d_{lm}). Fig.1 summarizes the coupling interactions until here described.

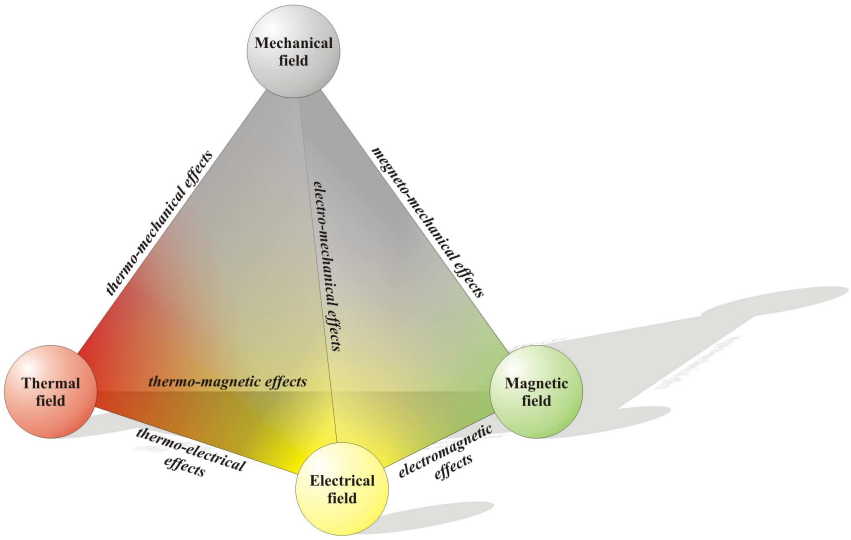

Figure 1. Interaction processes between the mechanical, thermal, electrical, and magnetic fields

III. Variational statements

As stated in a previous work,[8] piezoelectricity is based on a quasi-static approximation.[9] This approximation can be considered as the lowest order approximation of a perturbation procedure based on the fact that the acoustic wave speed is much smaller than the speed of the light. The same is for magneto-mechanical phenomena. As a result of this approximation, in the theory of piezoelectricity, although the mechanical equations are dynamic, the electromagnetic equations are static and the electric field and the magnetic field are not dynamically coupled. Therefore the wave behavior of electromagnetic field is not described. For many applications of piezoelectric acoustic wave devices, the quasi-static theory is sufficient, but there are situations in which full electromagnetic coupling needs to be considered. For example, electromagnetic waves generated by mechanical field need to be studied in the calculation of radiated electromagnetic power from a piezoelectric device. Full Maxwell equations also need to be considered in devices in which acoustic waves

produce electromagnetic waves or vice versa. More in general, when electromagnetic waves are involved, the complete set of Maxwell equations needs to be used, coupled to the mechanical equations of motion. In that way a fully dynamic theory can be obtained. An interesting discussion on that topic has been recently provided by Yang in the already mentioned work.[8] However, in the present work, electric field and magnetic field are considered not dynamically coupled.

A. Extension of PVD to multifield problems

In this section the Principle of Virtual Displacements (PVD) is derived for the full case. It means that complete coupling among mechanical, thermal, electrical and magnetic variables is considered. It is convenient to start the derivation directly from Hamilton's principle:

$$\delta \int_{t_0}^{t} (K - \Pi)\, dt \;=\; 0 \qquad \Rightarrow \qquad \delta \int_{t_0}^{t} K\, dt - \delta \int_{t_0}^{t} \Pi\, dt \;=\; 0, \tag{11}$$

where K is the kinetic energy and Π is the potential energy; δ is the variational symbol; t denotes time, t_0 and t_1 are the initial and generic instant. The kinetic energy variation can be treated as it follows:

$$\delta \int_{t_0}^{t} K\, dt \;=\; \delta \int_{t_0}^{t} dt \int_V \Big(\frac{1}{2}\,\rho\,\dot{u}_i\,\dot{u}_i\Big)\, dV \;=\; \int_{t_0}^{t} \int_V \rho\,\dot{u}_i\,\delta\dot{u}_i\, dV\, dt \;=\; \int_V \rho\,\dot{u}_i\,\delta u_i\, dV\Big|_{t_0}^{t_1} \;-\; \int_{t_0}^{t_1} \int_V \rho\,\ddot{u}_i\,\delta u_i\, dV\, dt. \tag{12}$$

V is the plate volume, u_i is a displacement component and dot denotes differentiation with respect to time. δu is equal zero in $t = t_0$ and $t = t_1$, so that:

$$\delta \int_{t_0}^{t} K\, dt \;=\; -\int_{t_0}^{t_1} \int_V \rho\,\ddot{u}_i\,\delta u_i\, dV\, dt \qquad \Rightarrow \qquad \delta \int_{t_0}^{t} K\, dt \;=\; -\int_{t_0}^{t} \delta L_{in}\, dt, \tag{13}$$

in which δL_{in} denotes the variation of the work done by inertial forces.
The variation of potential energy is written as algebraic sum of the variation of the Gibbs free energy and the variation of the work made by applied mechanical, thermal and electrical loading. Any hypothetical load due to magnetic field is here neglected. For practical reasons, body forces and volumetric electrical charges are neglected too:

$$\delta \int_{t_0}^{t} \Pi\, dt \;=\; \delta \int_{t_0}^{t} \left[\int_V G\, dV - \int_A \left(\bar{t}_j\, u_j - \bar{Q}\,\Phi\right)\, dA\right] dt \;=\; \delta \int_{t_0}^{t} \int_V G\, dV\, dt - \int_{t_0}^{t} \delta L_e\, dt, \tag{14}$$

where:
A is the surface involved by loading;
$\bar{t}_j$ is the mechanical loading in j-direction;
$\bar{Q}$ is the charge density on the plate surface;
ϕ is the electric potential;
δL_e denotes the variation of the work done by external loads.

Upon substitution of Eq.(13) and Eq.(14) in Eq.(11) it follows that:

$$\delta \int_{t_0}^{t} \int_V G\, dV\, dt \;=\; \int_{t_0}^{t} \delta L_e\, dt - \int_{t_0}^{t} \delta L_{in}\, dt. \tag{15}$$

Differentiating the Gibbs free energy, Eq.(15) takes the following form:

$$\int_{t_0}^{t} \int_V \Big(\frac{\partial G}{\partial \epsilon_{ij}}\delta\epsilon_{ij} + \frac{\partial G}{\partial T}\delta T + \frac{\partial G}{\partial E_l}\delta E_l + \frac{\partial G}{\partial H_l}\delta H_l\Big)\, dV\, dt = \int_{t_0}^{t} \delta L_e\, dt - \int_{t_0}^{t} \delta L_{in}\, dt. \tag{16}$$

Upon substitution of Eqs.4, by eliminating the time integral, the PVD for a three-dimensional continua is obtained:

$$\int_V (\sigma_{ij}\delta\epsilon_{ij} - \eta\delta\theta - D_l\delta E_l - B_l\delta H_l)\, dV \;=\; \delta L_e - \delta L_{in}. \tag{17}$$

1. Use of condensed notation

Passing from indices to vectors, it is useful to collect vectors $\boldsymbol{\sigma}, \mathbf{D}, \mathbf{B}, \eta$ and $\boldsymbol{\epsilon}, \mathbf{E}, \mathbf{H}, \theta$ in $\boldsymbol{\mathcal{E}}$ and $\boldsymbol{\mathcal{S}}$ respectively; $\boldsymbol{\mathcal{S}}$ is the vector of extensive variables while $\boldsymbol{\mathcal{E}}$ is the vector of intensive ones (bold letters denote arrays and ϵ_{ij} components in vectorial notation correspond to $2\epsilon_{ij}$ components in tensorial notation, when $i \neq j$):

$$\boldsymbol{\mathcal{S}}^T = \left\{ \begin{array}{cccccccccccccc} \sigma_{11} & \sigma_{22} & \sigma_{12} & D_1 & D_2 & B_1 & B_2 & \eta & \sigma_{33} & \sigma_{13} & \sigma_{23} & D_3 & B_3 \end{array} \right\}, \tag{18}$$

$$\boldsymbol{\mathcal{E}}^T = \left\{ \begin{array}{cccccccccccccc} \epsilon_{11} & \epsilon_{22} & \epsilon_{12} & E_1 & E_2 & H_1 & H_2 & \theta & \epsilon_{33} & \epsilon_{13} & \epsilon_{23} & E_3 & H_3 \end{array} \right\}. \tag{19}$$

Note that dealing with plates, subscript "3" indicates the through-the-thickness plate z-direction while subscripts "1" and "2" are for the remaining 2 orthogonal in-plane directions. By using these two vectors, the PVD statement for a multilayered plate results in the following compact form:

$$\int_V \left(\delta \boldsymbol{\mathcal{E}}_G^T \boldsymbol{\mathcal{S}}_H \right) dV \; = \; \delta L_e - \delta L_{in}, \tag{20}$$

where subscripts "G" and "H" indicates variables obtained by Geometrical relations and by constitutive/Hooke's relations respectively. For multilayered structures, the volume integral, has to be intended as:

$$\int_V (...) \; dV \; = \; \sum_{k=1}^{N_l} \int_{\Omega_k} \int_{h_k} (...) \; d\Omega_k \, dz, \tag{21}$$

where Ω_k is the layer middle surface, h_k denotes the k-layer thickness domain and N_l indicates the number of layers.

2. Particular cases

PVD in Eq.(20) can also be written in the following form:

$$\int_V \delta \boldsymbol{\epsilon}_{pG}^T \boldsymbol{\sigma}_{pH} + \delta \boldsymbol{\epsilon}_{nG}^T \boldsymbol{\sigma}_{nH} - \delta \boldsymbol{H}_{pG}^T \boldsymbol{B}_{pH} - \delta H_{nG} B_{nH} - \delta \boldsymbol{E}_{pG}^T \boldsymbol{D}_{pH} - \delta E_{nG} D_{nH} - \delta \theta_G \eta_H \, dV \; = \; \delta L_e - \delta L_{in}, \tag{22}$$

where notation already used in previous work[5] is referred to: subscript "p" denotes in-plane unknowns and subscript "n" denotes out-of-plane unknowns. In practical applications, not all the intensive variables (θ, ϵ, E, H) are taken as independent. Considering all the possible combinations of virtual variation active in the model, many different governing equations can be obtained. For the PVD, virtual variations here addressed to are six: δu_1, δu_2, δu_3, $\delta\phi$, $\delta\varphi$, $\delta\theta$; where $\delta\phi$ and $\delta\varphi$ indicate the variations of electric and magnetic potential, respectively[a]. In general, a virtual variation can be considered alone or can be coupled with the others. A few examples of variational statements for different case of coupling are proposed in the following. Reference is made to the form of PVD at Eq.(22). Six additional PVD forms are discussed.

PVD-1: Pure Mechanical case. If only virtual variations of displacements δu_1, δu_2, δu_3 are considered, Eq.(17) is reduced to:

$$\int_V \delta \boldsymbol{\epsilon}_{pG}^T \boldsymbol{\sigma}_{pH} + \delta \boldsymbol{\epsilon}_{nG}^T \boldsymbol{\sigma}_{nH} \, dV \; = \; \delta L_e - \delta L_{in}. \tag{23}$$

That is a pure mechanical problem is described.

PVD-2: Coupled Thermo-Mechanical case. By adding the variation of temperature: δu_1, δu_2, δu_3, $\delta\theta$, Eq.(17) becomes:

$$\int_V \delta \boldsymbol{\epsilon}_{pG}^T \boldsymbol{\sigma}_{pH} + \delta \boldsymbol{\epsilon}_{nG}^T \boldsymbol{\sigma}_{nH} - \delta \theta_G \eta_H \, dV \; = \; \delta L_e - \delta L_{in}. \tag{24}$$

That is a coupled thermo-mechanical problem is described.

PVD-3: Partially coupled Thermo-Mechanical case.

[a] To be noticed that δu_1, δu_2, δu_3 come from the strain $\delta\epsilon$, $\delta\phi$ from δE and $\delta\varphi$ from δH.

By saying that thermal field is partially coupled with mechanical field, it is intended that the extensive variable concerning thermal field (η) is not considered in constitutive relations. The thermal field impacts the system under form of thermal stresses σ_θ and thermal load vector. The advantage of using a partially coupled system lies in the reduction of the number of system degrees of freedoms. The disadvantage is that thermal effect due to strain is neglected and the temperature must be known in any point of the considered continuum. Corresponding Eq.(17) is:

$$\int \delta\boldsymbol{\epsilon}_{pG}^T(\boldsymbol{\sigma}_{pH} - \boldsymbol{\sigma}_{p\theta}) + \delta\boldsymbol{\epsilon}_{nG}^T(\boldsymbol{\sigma}_{nH} - \boldsymbol{\sigma}_{n\theta})\, dV \;=\; \delta L_e - \delta L_{in}. \tag{25}$$

PVD-4: Coupled Electro-Mechanical case. The considered virtual variations are: δu_1, δu_2, δu_3, $\delta\phi$ and the PVD reduces to:

$$\int_V \delta\boldsymbol{\epsilon}_{pG}^T\boldsymbol{\sigma}_{pH} + \delta\boldsymbol{\epsilon}_{nG}^T\boldsymbol{\sigma}_{nH} - \delta\boldsymbol{E}_{pG}^T\boldsymbol{D}_{pH} - \delta E_{nG}D_{nH}\, dV \;=\; \delta L_e - \delta L_{in}. \tag{26}$$

PVD-5: Coupled Magneto-Mechanical case. The considered virtual variations are: δu_1, δu_2, δu_3, $\delta\varphi$ and the PVD reduces to:

$$\int_V \delta\boldsymbol{\epsilon}_{pG}^T\boldsymbol{\sigma}_{pH} + \delta\boldsymbol{\epsilon}_{nG}^T\boldsymbol{\sigma}_{nH} - \delta\boldsymbol{H}_{pG}^T\boldsymbol{B}_{pH} - \delta H_{nG}B_{nH}\, dV \;=\; \delta L_e - \delta L_{in}. \tag{27}$$

PVD-6: Coupled Magneto-Electro-Mechanical case. The considered virtual variations are: δu_1, δu_2, δu_3, $\delta\phi$, $\delta\varphi$ and the PVD statement is:

$$\int_V \delta\boldsymbol{\epsilon}_{pG}^T\boldsymbol{\sigma}_{pH} + \delta\boldsymbol{\epsilon}_{nG}^T\boldsymbol{\sigma}_{nH} - \delta\boldsymbol{H}_{pG}^T\boldsymbol{B}_{pH} - \delta H_{nG}B_{nH} - \delta\boldsymbol{E}_{pG}^T\boldsymbol{D}_{pH} - \delta E_{nG}D_{nH}\, dV \;=\; \delta L_e - \delta L_{in}.$$

IV. FE equations in terms of "Fundamental Nuclei"

In the context of the so-called axiomatic approaches, where displacements or, more in general, stress field, thermal, electrical or magnetic variables are postulated in the thickness plate z-direction, two-dimensional theories are usually constructed accordingly to the following four steps.

I. Material behavior is assigned, i.e. constitutive relations are given (see Sec. II).

II. An appropriate variational statement (e.g. the PVD in Sec. III or the RMVT[b])[2] is used to establish governing equations and boundary conditions which are variationally consistent with the hypotheses introduced at points I,II,IV,V.

III. Geometrical relations (e.g. strain-displacement relations are assumed in the mechanical case).

IV. Displacement, stress distribution, electrical or magnetic variables in the thickness plate z-direction are *postulated* by referring to a certain set of base functions.

A. PVD - applications

1. Geometrical relation

$\boldsymbol{U}^k$ denotes the vector containing primary unknowns of the problem. Superscripts k and T indicates the k^{th} layer of the plate and the array transposition respectively. A suitable choice for PVD application is:

$$\boldsymbol{U}^{kT} = \left\{ \begin{array}{cccccc} u_1^k & u_2^k & u_3^k & \phi^k & \varphi^k & \theta^k \end{array} \right\}. \tag{28}$$

The intensive variables $\boldsymbol{\mathcal{E}}^k$ are linearly related to the unknowns $\boldsymbol{U}^k$ according to the following geometrical relations:

$$\boldsymbol{\mathcal{E}}_G^k = \boldsymbol{D}\boldsymbol{U}^k, \tag{29}$$

[b] Acronym of Reissner's Mixed Variational Theorem.

where $\boldsymbol{D}$ denotes the following differential operator:

$$\boldsymbol{D} = \begin{pmatrix} \partial_x & 0 & 0 & 0 & 0 & 0 \\ 0 & \partial_y & 0 & 0 & 0 & 0 \\ \partial_y & \partial_x & 0 & 0 & 0 & 0 \\ 0 & 0 & 0 & -\partial_x & 0 & 0 \\ 0 & 0 & 0 & -\partial_y & 0 & 0 \\ 0 & 0 & 0 & 0 & -\partial_x & 0 \\ 0 & 0 & 0 & 0 & -\partial_y & 0 \\ 0 & 0 & 0 & 0 & 0 & 1 \\ 0 & 0 & \partial_z & 0 & 0 & 0 \\ \partial_z & 0 & \partial_x & 0 & 0 & 0 \\ 0 & \partial_z & \partial_y & 0 & 0 & 0 \\ 0 & 0 & 0 & -\partial_z & 0 & 0 \\ 0 & 0 & 0 & 0 & -\partial_z & 0 \end{pmatrix}. \tag{30}$$

2. Constitutive relations

The lamina are considered to be homogeneous and to operate in the linear elastic range. Material is assumed to be orthotropic. Once rotated in the laminate reference system and considering the four-field linear coupling, constitutive coefficient can be organized in matrix $\boldsymbol{H}^k$:

$$\boldsymbol{\mathcal{S}}_H^k = \boldsymbol{H}^k \boldsymbol{\mathcal{E}}_G^k, \tag{31}$$

where:

$$\boldsymbol{H}^k = \begin{pmatrix} C_{11}^k & C_{12}^k & C_{16}^k & 0 & 0 & 0 & 0 & -\lambda_1^k & C_{13}^k & 0 & 0 & -e_{31}^k & -q_{31}^k \\ C_{12}^k & C_{22}^k & C_{26}^k & 0 & 0 & 0 & 0 & -\lambda_2^k & C_{23}^k & 0 & 0 & -e_{32}^k & -q_{32}^k \\ C_{16}^k & C_{26}^k & C_{66}^k & 0 & 0 & 0 & 0 & 0 & C_{36}^k & 0 & 0 & -e_{36}^k & -q_{36}^k \\ 0 & 0 & 0 & \varepsilon_{11}^k & \varepsilon_{12}^k & d_{11}^k & d_{12}^k & 0 & 0 & e_{15}^k & e_{14}^k & 0 & 0 \\ 0 & 0 & 0 & \varepsilon_{12}^k & \varepsilon_{22}^k & d_{12}^k & d_{22}^k & 0 & 0 & e_{25}^k & e_{24}^k & 0 & 0 \\ 0 & 0 & 0 & d_{11}^k & d_{12}^k & \mu_{11}^k & \mu_{12}^k & 0 & 0 & q_{15}^k & q_{14}^k & 0 & 0 \\ 0 & 0 & 0 & d_{12}^k & d_{22}^k & \mu_{12}^k & \mu_{22}^k & 0 & 0 & q_{25}^k & q_{24}^k & 0 & 0 \\ \lambda_1^k & \lambda_2^k & 0 & 0 & 0 & 0 & 0 & (\frac{\rho C}{\theta_{ref}})^k & \lambda_3^k & 0 & 0 & p_3^k & r_3^k \\ C_{13}^k & C_{23}^k & C_{36}^k & 0 & 0 & 0 & 0 & -\lambda_3^k & C_{33}^k & 0 & 0 & -e_{33}^k & -q_{33}^k \\ 0 & 0 & 0 & -e_{15}^k & -e_{25}^k & -q_{15}^k & -q_{25}^k & 0 & 0 & C_{55}^k & C_{45}^k & 0 & 0 \\ 0 & 0 & 0 & -e_{14}^k & -e_{24}^k & -q_{14}^k & -q_{24}^k & 0 & 0 & C_{45}^k & C_{44}^k & 0 & 0 \\ e_{31}^k & e_{32}^k & e_{36}^k & 0 & 0 & 0 & 0 & p_3^k & e_{33}^k & 0 & 0 & \varepsilon_{33}^k & d_{33}^k \\ q_{31}^k & q_{32}^k & q_{36}^k & 0 & 0 & 0 & 0 & r_3^k & q_{33}^k & 0 & 0 & d_{33}^k & \mu_{33}^k \end{pmatrix}. \tag{32}$$

3. Through-the-thickness assumptions for primary variables

In the framework of the CUF,[10] the primary unknowns are assumed by using a generalized expansion:

$$\boldsymbol{U}^k(x,y,z) = F_\tau(z)\, \boldsymbol{U}_\tau^k(x,y) \quad \tau = 0,1,...,N. \tag{33}$$

The repeated indexes are summed over their ranges. The polynomials $F_\tau(z)$ constitute a set of independent functions. Such a base are arbitrarily chosen: power of z, Lagrange polynomials or a combination of Legendre polynomials can be considered. N denotes the order of the introduced expansion. Note that the variables concerning displacements, electrical potential, magnetic potential and temperature are included in vector $\boldsymbol{U}^k$.

It is understood that, by the arbitrary choice of the thickness expansion, the same computational code can address not just one finite element, but a complete family of them, with different descriptions for primary

unknowns along the thickness of the structure. In so doing, the CUF reduces a three-dimensional problem to a two-dimensional problem. Meanwhile, the order of the expansion along the thickness of the plate is taken as a free parameter of the finite element and it can be changed ranging from 1 up to 4.
By appropriately choosing the thickness functions, both an Equivalent Single Layer (ESL) and Layer Wise (LW) description along the thickness of the plate is admissible. In an ESL model, a global assumption for the unknowns is considered along the thickness of the plate (i.e. a Taylor expansion) while in a LW model the expansion is made for each layer separately and then interlaminar continuity conditions are enforced by the assembly procedure. The latter leads generally to more accurate results but the number of the nodal degrees of freedom increases with the number of the layers coming out to a greater computational cost.
In the implemented code, for a LW theory the thickness functions are defined by:

$$F_t = \frac{P_0 + P_1}{2}, \quad F_b = \frac{P_0 - P_1}{2}, \quad F_r = P_r - P_{r-2} \quad r = 2, \ldots, N, \tag{34}$$

where $P_i = P_i(\zeta_k)$ is the *Legendre* polynomial of i^{th} order defined in the domain $-1 \leq \zeta_k \leq 1$. The chosen thickness functions have the interesting properties:

$$\zeta_k = \begin{cases} 1: & F_t = 1, \quad F_b = 0, \quad F_r = 0 \\ -1: & F_t = 0, \quad F_b = 1, \quad F_r = 0 \end{cases}. \tag{35}$$

Using these definitions, the generalized assumptions for the primary unknowns of the k^{th} layer in Eq.(33) can be stated as:

$$\boldsymbol{U}^{\,k}(x,y,z) = F_b(z)\boldsymbol{U}^{\,k}_{\,b}(x,y) + F_r(z)\boldsymbol{U}^{\,k}_{\,r}(x,y) + F_t(z)\boldsymbol{U}^{\,k}_{\,t}(x,y) = F_\tau \boldsymbol{U}^{\,k}_{\,\tau}, \quad \text{with} \quad r = 2, \ldots, N, \tag{36}$$

The the variables $\boldsymbol{U}_{\,b}$ and $\boldsymbol{U}_{\,t}$ are the actual primary unknowns at the bottom and the top surfaces of the layer and the inter-laminar continuity can be easily imposed:

$$\boldsymbol{U}^{\,k}_{\,t} = \boldsymbol{U}^{\,(k+1)}_{\,b}, \quad \text{with} \quad k = 1, \ldots, N_l - 1. \tag{37}$$

Acronyms are used for the implemented plate elements. These are denoted by LD1, LD2, LD3, LD4 in which: L states that a Layer-Wise description is employed and D indicates that classical approach based on PVD is used; 1-4 denotes the order of the expansion introduced for the field variables in each layer (from first to fourth order). When acronyms ED1, ED2, ED3, ED4 are used, an Equivalent-Single-Layer description is employed.

4. Finite element discretization

In case of FEM (Finite Element Method) implementation, unknowns can be expressed in terms of their nodal values, via the shape functions N_i:

$$\boldsymbol{U}^k_\tau(x,y) = N_i(x,y)\boldsymbol{Q}^k_{\tau i} \quad i = 1, 2, ..., N_n, \tag{38}$$

where N_n denotes the number of nodes of the considered finite element and $\boldsymbol{Q}^k_{\tau i}$ is the vector of the nodal values of the primary unknowns:

$$\boldsymbol{Q}^{kT}_{\tau i} = \left\{ \begin{array}{cccccc} Q^k_{u_1\tau i} & Q^k_{u_2\tau i} & Q^k_{u_3\tau i} & Q^k_{\phi\tau i} & Q^k_{\varphi\tau i} & Q^k_{\theta\tau i} \end{array} \right\}. \tag{39}$$

Substituting Eq.(38) in Eq.(33), the final expression of primary unknowns can be obtained:

$$\boldsymbol{U}^k(x,y,z) = F_\tau N_i \boldsymbol{Q}^k_{\tau i}. \tag{40}$$

5. Fundamental Nucleus

Upon substitution of what at Eqs.(29), (31), (33) and (38), the variational statement in Eq.(20) leads to a set of equilibrium equations which can be formally put in the following compact form:

$$\delta \boldsymbol{Q}^k_\tau : \quad \boldsymbol{K}^{k\tau sij}_{PVD}\, \boldsymbol{Q}^k_{sj} \;=\; \boldsymbol{P}^k_{\tau i}, \tag{41}$$

where $\boldsymbol{P}^k$ is the vector of external and inertial loads. The related boundary conditions are:

$$\boldsymbol{Q}_\tau^k = \overline{\boldsymbol{Q}}_\tau^k. \tag{42}$$

The number of obtained equations coincides with the number of introduced variables: τ and s vary from 0 to N, i and j vary from 1 to N_n and k ranges from 1 to N_l. Matrix $\boldsymbol{K}_{PVD}^{k\tau sij}$ is the so-called fundamental nucleus and, in this case, it is a 6×6 array.
Fundamental nuclei related to PVD-1$\div$ PVD-6 can be obtained as particular cases of Eq.(41). More details can be found in a DIASP internal report.[11]

V. FE problem

Whatever is the considered variational statement, for a given discretization, mass matrix $\boldsymbol{M}$ and stiffen matrix $\boldsymbol{K}$ can be calculated by numerical integration and the assembly procedure. This two matrices are representative of inertial and Gibbs free energy contribution respectively. It should be emphasized that the stiffen matrix, regardless its name, contains information pertaining to all the considered fields and not just to the mechanical field. On the contrary, the mass matrix concerns just the mechanical field. In fact, apart the mass, there are not other physical quantity related to the second time derivative of primary unknowns, when defining the kinetic energy.
The undamped dynamic problem now can be written in terms of the following ODE system:

$$\boldsymbol{M}\ddot{\boldsymbol{Q}} + \boldsymbol{K}\boldsymbol{Q} = \boldsymbol{F}, \tag{43}$$

where:
$\boldsymbol{Q}$ is the vector of nodal primary unknowns;
$\boldsymbol{F}$ is the vector of nodal loads.
Moreover, the i^{th} natural frequency of the system ω_i can be calculated by solving the generalized eigenvalues problem:

$$(-\omega_i^2\boldsymbol{M}+\boldsymbol{K})\boldsymbol{a_i} = \boldsymbol{0}, \tag{44}$$

where $\boldsymbol{a_i}$ is the i^{th} eigenvector.
If a static analysis is required, the system to solve is the following:

$$\boldsymbol{K}\boldsymbol{Q} = \boldsymbol{F}. \tag{45}$$

VI. Numerical results

This section shows several numerical results employed to assess the developed Finite Elements (FEs) for magneto-electro-thermo-elastic plate problems based on the PVD statement. For every case of analysis, a critical comparison between numerical results and exact solutions available in literature is presented. Results are obtained in MUL2, which is a Fortran-developed FEM code implemented accordingly to the here presented formulation. The reduced integration scheme has been preserved as done in several past studies.[12] Simple and regular mesh are considered.

A. Pure mechanical case: convergence study for the dynamic case (PVD-1)

A fully simply supported square plate of aluminium alloy 2024-T6 is considered under PVD analysis with a regular mesh of nine-nodes Quadrangular FEs (Q9), where a regular mesh is a mesh with the same number of equally-spaced elements along the two plate's directions. Material properties are those in Tab.1. The plate

	$E[GPa]$	$G[GPa]$	$\nu_{12}[-]$	$\rho[kg/m^3]$
Al 2024-T6	73	27.239	0.34	2800

Table 1. Material properties of the aluminium alloy Al 2024-T6

thickness ratio is 1/100. A fourth order through-the-thickness expansion for primary variables is considered

and the ESL theory is employed (the corresponding acronym for the FE is now ED4). In the following there is a comparison between the undamped natural frequencies calculated by FEM, in MUL2, and the ones calculated analytically. Frequencies ($\overline{\omega}$) are dimensionless accordingly to $\overline{\omega} = \omega\sqrt{a^4\rho/(h^2E_2)}$, where a is the plate side length, ρ is the material density, h is the thickness and E_2 is the transverse Young's modulus. By comparison between analytical and FEM results, it is proved the convergence of MUL2 results to the analytical solution based on the same theory (see Tab.3 and Fig.3). Moreover, in Fig.2 it is showed that by the present formulation, it is possible to detect the so-called thickness modes.

frequency number	*analytical*	FEM (mesh)		
		(3×3)	(6×6)	(9×9)
1	6.0570	6.0701	6.0578	6.0572
2	15.134	15.563	15.163	15.140
3	15.134	15.563	15.163	15.140
4	24.202	24.968	24.254	24.212

Table 2. Plate undamped dimensionless natural frequencies calculated for the pure mechanical case: convergence study of the Q9 ED4 finite element to the corresponding analytical solution - see the graphic view in Fig.3

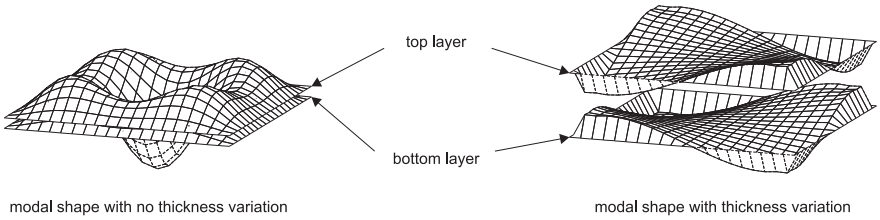

Figure 2. Two modal shapes of a plate: the right picture emphasizes the capability of present theory (two-dimensional modeling formulation) to catch the tree-dimensional effects

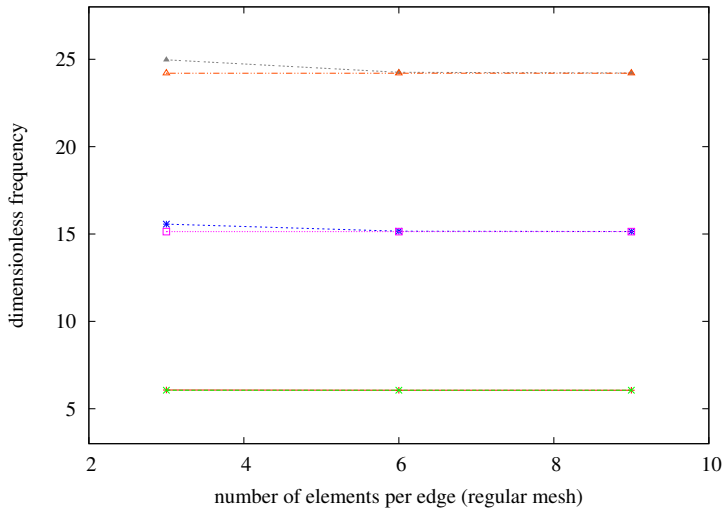

Figure 3. Graphical view of the convergence study in Tab.2 for the first three frequencies; Q9 ED4 FEs are employed

B. Thermo-mechanical case: benchmark for static analysis (PVD-3)

In this section several FEM results of thermo-mechanical static analysis of multilayered anisotropic plates obtained in MUL2 are compared to the 3D exact solutions found by Bhaskar and Varadan.[13] Numerical

results are presented for the bending of a $(0°/90°/0°)$ square (a=b) laminate due to the temperature field given by

$$\theta = \overline{\theta}(2z/h)sin(\frac{\pi x}{a})sin(\frac{\pi y}{b}), \tag{46}$$

where h is the total thickness of the laminate. The following material properties, typical of high-modulus graphite/epoxy, are assumed:

$$E_L/E_T = 25;$$
$$G_{LT}/E_T = 0.5;$$
$$G_{TT}/E_T = 0.2;$$
$$\nu_{LT}/\nu_{TT} = 0.25;$$
$$\alpha_T/\alpha_L = 1125,$$

where L and T refer to directions parallel and perpendicular, respectively, to the fibres. In the FEM analysis, the dimensional values given for material properties are though coherently with the above given dimensionless ratios.

Note that the distribution of temperature along the thickness, for given thermal boundary conditions at the top and at the bottom surfaces, can be obtained by solution of the heat conduction equation (see, for example, the work of Tungikar and Rao[14]). However, only simple linear antisymmetric (with respect to z) thermal variation is considered as this would lead to bending (without stretching) of a symmetric laminate and would be adequate to bring out the importance of non-classical influences such as shear deformation and thickness stretch.

The deflections and stresses are presented in terms of the following dimensionless parameters (sign $\widetilde{}$):

$$\widetilde{u}_3 = \frac{u_3}{h\alpha_L\overline{\theta}S^2}, \qquad (\widetilde{u}_1, \widetilde{u}_2) = \frac{(u_1, u_2)}{h\alpha_L\overline{\theta}S}, \qquad \widetilde{\sigma}_{ij} = \frac{\sigma_{ij}}{E_T\alpha_L\overline{\theta}},$$

with $S = a/h$.

In Tabs.3,4 there is a comparisons between the 3D exact solution of the above described problem[13] and the FEM results obtained by multifield FEs of different accuracy along the thickness: the acronym associated to the employed FEs is LDn, where L is for a Layer-Wise FE, D is for the PVD variational statement and n (in this case one or four) is the order of the thickness functions used. Results in Tab.3 are free of thickness locking since the reduction of the constitutive relations.[15] Even if the employed mesh is not particularly refined, LD4 FEM results are in very good agreement with the exact solution, both for displacement and for in-plane stresses. In the other side, results obtained by LD1 FEs are in general accurate only for thin plates. Results of the convergence study for displacements and for in-plane stresses can be found in Figs.4,5. It can be noticed that FEM solutions converge to the 3D exact values[13] and that accurate results for displacements and in-plane stresses are obtained by Q9 FEs even with a poor mesh. Moreover, it is conformed that the convergence is much faster for displacements than for stresses. More details on the thermo-mechanical coupling effect can be found in a previous work.[7]

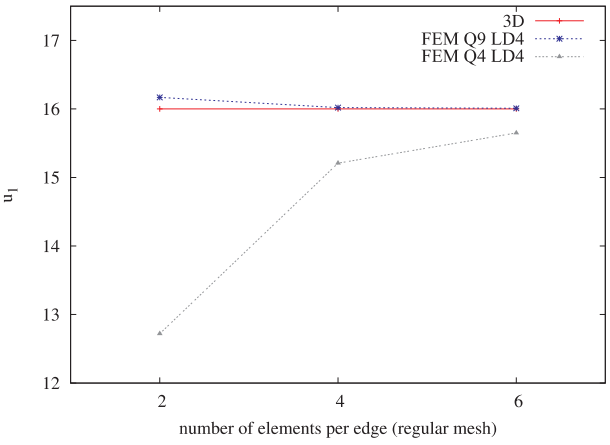

Figure 4. Convergence study for displacement u_1

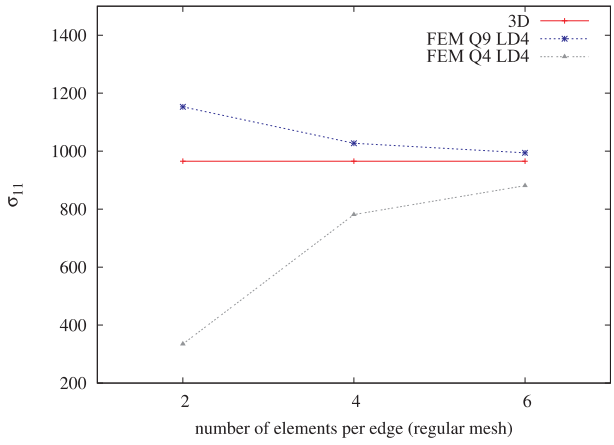

Figure 5. Convergence study for stress σ_{11}

S	*sol.*	$\widetilde{u}_1(\mp\frac{h}{2})$	$\widetilde{u}_2(\mp\frac{h}{2})$	$\widetilde{u}_3(\mp\frac{h}{2})$	$\widetilde{\sigma}_{11}(\pm\frac{h}{2})$	$\widetilde{\sigma}_{22}(\mp\frac{h}{2})$	$\widetilde{\sigma}_{12}(\mp\frac{h}{2})$
2	3D[13]	±20.04	±151.4	96.79	±1390	±635.4	±269.3
2	FEM	±12.88	±162.4	90.38	±672.3	±711.3	±281.5
4	3D[13]	±18.11	±81.83	42.69	±1183	±856.1	±157.0
4	FEM	±16.51	±86.08	41.82	±916.0	±960.2	±164.9
10	3D[13]	±16.61	±31.95	17.39	±1026	±1014	±76.29
10	FEM	±17.31	±33.47	17.84	±945.3	±1134	±81.65
20	3D[13]	±16.17	±20.34	12.12	±982.0	±1051	±57.35
20	FEM	±17.29	±21.59	12.82	±936.4	±1173	±62.55
50	3D[13]	±16.02	±16.71	10.50	±967.5	±1063	±51.41
50	FEM	±17.26	±17.92	11.27	±931.7	±1186	±56.55
100	3D[13]	±16.00	±16.17	10.26	±965.4	±1065	±50.53
100	FEM	±17.25	±17.40	11.05	±930.1	±1187	±55.65
CLT	EX.[13]	±15.99	±15.99	10.18	±964.6	±1065	±50.24

Table 3. z values are given in parentheses; (x, y) values are: $(a/2, a/2)$ for $\widetilde{u}_3$, $\widetilde{\sigma}_{11}$ and $\widetilde{\sigma}_{22}$; $(0, a/2)$ for $\widetilde{u}_1$; $(a/2, 0)$ for $\widetilde{u}_2$ and $(0, 0)$ for $\widetilde{\sigma}_{12}$ - a regular 6×6 mesh of Q9 LD1 FEs is employed with thickness locking correction

S	*sol.*	$\widetilde{u}_1(\mp\frac{h}{2})$	$\widetilde{u}_2(\mp\frac{h}{2})$	$\widetilde{u}_3(\mp\frac{h}{2})$	$\widetilde{\sigma}_{11}(\pm\frac{h}{2})$	$\widetilde{\sigma}_{22}(\mp\frac{h}{2})$	$\widetilde{\sigma}_{12}(\mp\frac{h}{2})$
2	3D[13]	±20.04	±151.4	96.79	±1390	±635.4	±269.3
2	FEM	±20.09	±151.4	96.74	±1432	±624.2	±275.3
4	3D[13]	±18.11	±81.83	42.69	±1183	±856.1	±157.0
4	FEM	±18.16	±81.82	42.68	±1220	±850.2	±160.5
10	3D[13]	±16.61	±31.95	17.39	±1026	±1014	±76.29
10	FEM	±16.66	±31.91	17.39	±1059	±1012	±78.05
20	3D[13]	±16.17	±20.34	12.12	±982.0	±1051	±57.35
20	FEM	±16.21	±20.29	12.12	±1013	±1050	±58.69
50	3D[13]	±16.02	±16.71	10.50	±967.5	±1063	±51.41
50	FEM	±16.05	±16.68	10.50	±997.4	±1061	±52.58
100	3D[13]	±16.00	±16.17	10.26	±965.4	±1065	±50.53
100	FEM	±16.01	±16.16	10.26	±994.3	±1063	±51.66
CLT	EX.[13]	±15.99	±15.99	10.18	±964.6	±1065	±50.24

Table 4. z values are given in parentheses; (x, y) values are: $(a/2, a/2)$ for $\widetilde{u}_3$, $\widetilde{\sigma}_{11}$ and $\widetilde{\sigma}_{22}$; $(0, a/2)$ for $\widetilde{u}_1$; $(a/2, 0)$ for $\widetilde{u}_2$ and $(0, 0)$ for $\widetilde{\sigma}_{12}$ - a regular 6×6 mesh of Q9 LD4 FEs is employed

C. Thermo-mechanical case: coupled static analysis (PVD-2)

A simply supported square aluminum plate is studied to investigate about the coupling between temperature and mechanical fields. In the authors' knowledge a benchmark for such analyses is not available in literature thus the analysis of a simple isotropic plate is proposed. Results are shown in dimensional form so that numbers can be judjed by engineering sense.
The mechanical properties are:

$$E = 73[GPa]; \qquad \nu = 0.3; \qquad \alpha = 25E - 6\left[K^{-1}\right]; \qquad C = 897\left[\frac{J}{kgK}\right]; \qquad \rho = 2800\left[\frac{kg}{m^3}\right].$$

The plate dimensions are: length and width $a = b = 10\ [m]$, thickness $h = 1\ [m]$. The plate has been loaded by the bi-sinusoidal pressure:

$$p = \frac{2\,p_m\,z}{h}\sin\left(\frac{\pi\,x}{a}\right)\sin\left(\frac{\pi\,y}{b}\right), \tag{47}$$

where the peak value is $p_m = 200\ [MPa]$. A sketch can be seen in Fig.(6).

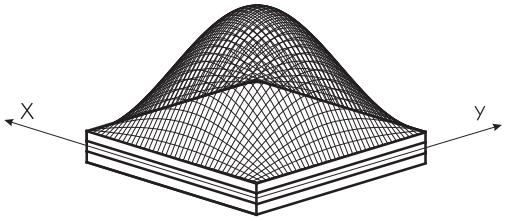

Figure 6. Load and plate configuration

A 6×6 mesh of LD4 Q9 elements is employed. The comparison between full thermal analysis and simple mechanical analysis is shown in Figs.7-9 for the three displacements. It can be noted that there is not substantial difference in terms of displacements between those two analysis. A slight difference can be seen in Fig.9 for displacement u_3, but anyway such distinction is still very small. The fact is that for a fully coupled thermo-mechanical analysis, only a small part of work is employed to modify the temperature of the plate. The u_3 displacement for this kind of analysis results to be smaller than the one obtained by a simple mechanical analysis because a part of work is used to develop the temperature variation. The same amount of work is subtracted from the work used to deform the plate. It can be seen that only a small part of work has been used to modify the temperature. In fact, the maximum value of thermal variation is 0.02 $[K]$. Normal stresses have been calculated successfully using both the analysis. See the previous work[7] for more details.

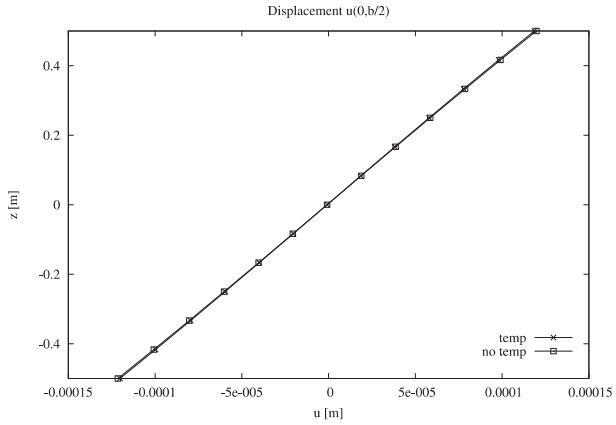

Figure 7. $u_1(0, \frac{b}{2})$**,** 6×6 **mesh, LD4 Q9 elements**

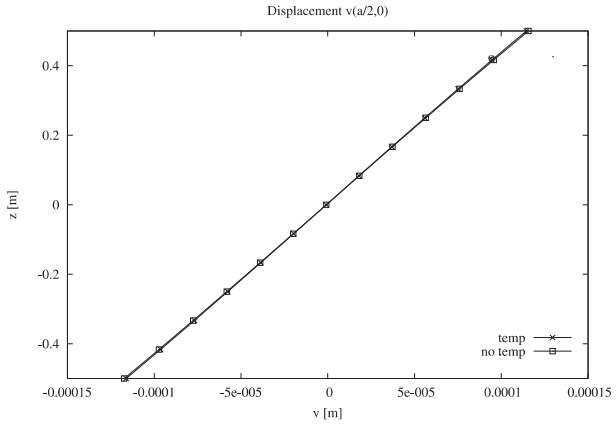

Figure 8. $u_2(\frac{a}{2}, 0)$**,** 6×6 **mesh, LD4 Q9 elements**

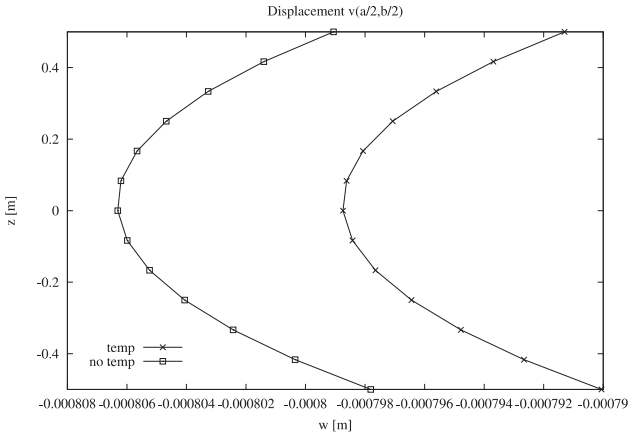

Figure 9. $u_3(\frac{a}{2}, \frac{b}{2})$, 6×6 **mesh, LD4 Q9 elements**

D. Electro-mechanical case: benchmark for static analysis (PVD-4)

In this section a few FEM results obtained in MUL2 are compared with the exact solution provided by Heyliger.[16] The laminate considered is a [0/90] cross-ply composed of an elastic material with piezoelectric layers bonded to the upper and lower surfaces. The plate is square of side length a. The total thickness is h. The elastic layers have thickness of $0.4h$, with the piezoelectric layer thicknesses of $0.1h$. The elastic material is modeled after a fiber-reinforced composite and has the properties $E_{11} = 132.38$ (all in $[GPa]$), $E_{22} = 10.756$, $E_{33} = 10.756$, $G_{44} = 3.606$, $G_{55} = 5.654$, $G_{66} = 5.654$, $\nu_{12} = 0.24$, $\nu_{13} = 0.24$, $\nu_{23} = 0.49$, $\varepsilon_{11}/\varepsilon_0 = 3.5$, and $\varepsilon_{22}/\varepsilon_0 = \varepsilon_{33}/\varepsilon_0 = 3.0$. The piezoelectric layers are modeled after PZT-4 and have the material properties $E_{11} = E_{22} = 81.3$ (all in $[GPa]$), $E_{33} = 64.5$, $G_{44} = G_{55} = 25.6$, $G_{66} = 30.6$, $\nu_{12} = 0.329$, $\nu_{13} = \nu_{23} = 0.432$, $e_{31} = e_{32} = -5.20$ (all in $[C/m^2]$), $e_{33} = 15.08$, $e_{24} = e_{15} = 12.72$, and $\varepsilon_{11}/\varepsilon_0 = \varepsilon_{11}/\varepsilon_0 = 1475$, $\varepsilon_{33}/\varepsilon_0 = 1300$. The piezoelectric layer thickness are taken as 0.1 $[m]$.
Both applied double sinusoidal pressure loading and double sinusoidal surface potential are considered at the top plate surface: sensor and actuator configuration respectively. See the two configuration in Fig.10, where p_z indicates a pressure $[N/m^2]$ and ϕ_t indicates the potential $[V]$ imposed at the top face and $\widehat{p}_z = \widehat{\phi}_t = 1$. The aspect ratio in both cases is $a/h = 4$. For the applied pressure load, the top and bottom laminate surfaces are fixed at zero potential. For the applied potential, these surfaces are stress free and the bottom surface is fixed to zero potential. FEM results are in Tabs.5,6.
Following consideration on the obtained results can be done: FEM results achieved by LW theory are in general more accurate respect to those achieved by the ESL theory. In particular, for displacements, LW results obtained with a first order through-the-thickness expansion are more accurate than ESL results obtained with a fourth order expansion. In addition, stress results provided by LW analysis are in good agreement with the exact solution, while the ESL theory can lead to significant errors. In conclusion, it has been showed that results provided by LW FEs based on the PVD statement are very close to exact solutions for both piezoelectric sensor and actuator cases. Anyway such a conclusion could not be extended to different plate problems or to results related to other variables evaluated in different points.

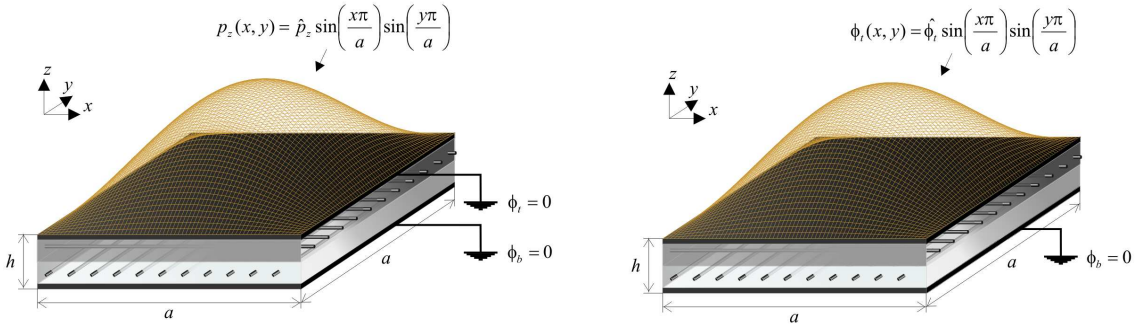

Figure 10. On the left the plate in sensor configuration (applied pressure); on the right the plate in actuator configuration (applied potential)

sol.	$u_2(\frac{a}{2},0,\frac{h}{2})$	$u_3(\frac{a}{2},\frac{a}{2},0)$	$\phi(\frac{a}{2},\frac{a}{2},0)$	$\sigma_{12}(0,0,\frac{h}{2})$	$\sigma_{22}(\frac{a}{2},\frac{a}{2},\frac{h}{2})$
3D[16]	-4.7549E-11	3.0027E-10	6.11E-3	-2.4776	6.5643
FEM LD1	-4.6171E-11	2.9848E-10	6.0111E-3	-2.4946	6.8348
FEM LD2	-4.7443E-11	2.9978E-10	6.1011E-3	-2.5255	6.2586
FEM LD3	-4.7628E-11	3.0025E-10	6.1173E-3	-2.5332	6.2642
FEM LD4	-4.7630E-11	3.0025E-10	6.1176E-3	-2.5332	6.2641
FEM ED1	-2.4461E-11	1.8446E-10	2.6635E-3	-1.6585	3.2675
FEM ED2	-3.1366E-11	2.0910E-10	6.2727E-3	-2.0879	1.1330
FEM ED3	-4.5036E-11	2.8497E-10	5.8379E-3	-2.5116	1.3953
FEM ED4	-4.7567E-11	2.8581E-10	6.1351E-3	-2.5286	1.8642

Table 5. Results pertaining to the sensor configuration; displacements are in $[m]$, the electric potential is in $[V]$ and stresses are in $[N/m^2]$

sol.	$u_2(\frac{a}{2},0,\frac{h}{2})$	$u_3(\frac{a}{2},\frac{a}{2},0)$	$\phi(\frac{a}{2},\frac{a}{2},0)$	$\sigma_{12}(0,0,\frac{h}{2})$	$\sigma_{22}(\frac{a}{2},\frac{a}{2},\frac{h}{2})$
3D[16]	-3.2764E-11	-1.4711E-11	4.476E-1	-1.4603	1.1181
FEM LD1	-2.3764E-11	-1.6965E-11	4.4693E-1	-1.2983	3.4555
FEM LD2	-2.2516E-11	-1.5490E-11	4.4805E-1	-1.2532	1.5853
FEM LD3	-2.2602E-11	-1.5560E-11	4.4801E-1	-1.2765	1.4782
FEM LD4	-2.2648E-11	-1.5580E-11	4.4801E-1	-1.2791	1.4598
FEM ED1	-2.9655E-11	-1.5005E-11	4.4621E-1	-2.7358	4.5438
FEM ED2	-1.9209E-11	-1.3684E-11	4.4879E-1	-1.2923	5.2010
FEM ED3	-3.2936E-11	-3.6096E-11	4.4822E-1	-1.7342	10.967
FEM ED4	-2.7908E-11	-3.3901E-11	4.4844E-1	-1.4429	11.580

Table 6. Results pertaining to the actuator configuration; displacements are in $[m]$, the electric potential is in $[V]$ and stresses are in $[N/m^2]$

E. Electro-magneto-mechanical case: benchmark for static analysis (PVD-6)

This section shows some numerical results obtained in MUL2 to assess the developed FEs for static magneto-electro-mechanical multilayered plate problems which are based on PVD's application.
Present FE analysis are compared with 3D exact solution by Pan.[17] Square plates which are loaded at the top layer surface and with simply supported edges are analyzed. Layered plates are build by using a combination of layers made of piezoelectric and magnetostrictive materials. The piezoelectric material consists of $BaTiO_3$ (called B for brevity) and the magnetostrictive one $CoFe_2O_4$ (called F for brevity). The physical properties of these two materials are given in Tab.7, where C_{ij}, e_{ij}, q_{ij} are the stiffness, piezoelectric and piezomagnetic coefficients while ε_{ij} and μ_{ij} are the electric permittivity and the magnetic permeability respectively. The considered stacking sequences are B/F/B and F/B/F, the load is a bi-sinusoidal pressure

Properties	$BaTiO_3$	$CoFe_2O_4$	Properties	$BaTiO_3$	$CoFe_2O_4$
C_{11}[GPa]	166	286	$e_{31}[C/m^2]$	-4.4	0
C_{22}[GPa]	166	286	$e_{32}[C/m^2]$	-4.4	0
C_{12}[GPa]	77	173	$e_{33}[C/m^2]$	18.6	0
C_{13}[GPa]	78	170.5	$e_{24}[C/m^2]$	11.6	0
C_{23}[GPa]	78	170.5	$e_{15}[C/m^2]$	11.6	0
C_{33}[GPa]	162	269.5	$q_{31}[N/(Am)]$	0	580.3
C_{44}[GPa]	43	45.3	$q_{32}[N/(Am)]$	0	580.3
C_{55}[GPa]	43	45.3	$q_{33}[N/(Am)]$	0	699.7
C_{66}[GPa]	44.5	56.5	$q_{24}[N/(Am)]$	0	550
			$q_{15}[N/(Am)]$	0	550
$\varepsilon_{11} \times 10^9[C^2/(Nm^2)]$	11.2	0.08			
$\varepsilon_{22} \times 10^9[C^2/(Nm^2)]$	11.2	0.08			
$\varepsilon_{33} \times 10^9[C^2/(Nm^2)]$	12.6	0.093			
$\mu_{11} \times 10^6[Ns^2/C^2]$	5	-590			
$\mu_{22} \times 10^6[Ns^2/C^2]$	5	-590			
$\mu_{33} \times 10^6[Ns^2/C^2]$	10	157			

Table 7. Properties of the materials employed in the reference work

of peak 1 $[N/m^2]$, applied at the top face; each layer has the same thickness $h_k = 0.1$ $[m]$, plate length is $a = 1$ $[m]$ and all the quantities have been calculated with correspondence to the in-plane coordinate values: $x = 0.75$ $[m]$ and $y = 0.25$ $[m]$, as done in the referenced article.[17]
LW and ESL results are here compared with the exact solution. Linear, parabolic, 3^{rd} and 4^{th} order LW and ESL results have been compared in Tabs.8-11.
At this point it is important to underline that in the FEM analysis the plate is considered as sensor. As a consequence of that, electric and magnetic potentials are set to zero at the top and at the bottom face. Since such boundary condition is not imposed in the exact solution, FEM and exact potentials values are not in agreement. Anyway, this discrepancy does not affect results related to other quantities.
Displacements calculated by ESL theory are often (but not always) close to the exact solution, but a high order through-the-thickness expansion is often required. With the LW approach good results for displacement can be reached even without a high order through-the-thickness expansion. In general, best results for stresses are obtained by LW theory with high order through-the-thickness expansion, while ESL approach can lead to unreasonable numbers. More details and results can be found in another work devoted to interactions between the magnetic field and the others.[18]

	$\sigma_{33}[Pa]$ top face	$\sigma_{13}[Pa]$ center	$u_1[m]$ bottom face	$u_3[m]$ bottom face
3D[17]	0.5	-3.96×10^{-1}	-2.01×10^{-12}	5.4×10^{-12}
FEM LD1	0.74	-4.14×10^{-1}	-2.02×10^{-12}	5.5×10^{-12}
FEM LD2	0.57	-4.31×10^{-1}	-2.05×10^{-12}	5.6×10^{-12}
FEM LD3	0.55	-4.24×10^{-1}	-2.05×10^{-12}	5.6×10^{-12}
FEM LD4	0.51	-4.23×10^{-1}	-2.05×10^{-12}	5.6×10^{-12}
FEM ED1	1.38	-1.94×10^{0}	-1.24×10^{-13}	5.7×10^{-12}
FEM ED2	3.95	-3.04×10^{-1}	-1.50×10^{-13}	6.4×10^{-12}
FEM ED3	2.96	-1.00×10^{0}	-1.44×10^{-13}	6.72×10^{-12}
FEM ED4	9.18	-4.78×10^{-2}	-1.45×10^{-13}	6.82×10^{-12}

Table 8. Comparison of various kinematics for the B/F/B plate: evaluation of transverse stresses and displacements

	$\phi_{MAX}[V]$	$\psi_{MAX}[C/s]$	$\sigma_{11}[Pa]$ top face	σ_{12}[Pa] bottom face
3D[17]	1.54×10^{-3}	-2.61×10^{-6}	1.27	-5.77×10^{-1}
FEM LD1	8.33×10^{-4}	-7.07×10^{-7}	1.43	-5.38×10^{-1}
FEM LD2	8.39×10^{-4}	-7.15×10^{-7}	1.39	-5.47×10^{-1}
FEM LD3	8.39×10^{-4}	-7.11×10^{-7}	1.38	-5.48×10^{-1}
FEM LD4	8.39×10^{-4}	-7.12×10^{-7}	1.38	-5.48×10^{-1}
FEM ED1	5.98×10^{-4}	-6.65×10^{-7}	2.67	-3.35×10^{-2}
FEM ED2	1.01×10^{-3}	-8.22×10^{-7}	4.39	-3.06×10^{-2}
FEM ED3	9.86×10^{-4}	-8.08×10^{-7}	5.76	-3.02×10^{-2}
FEM ED4	9.97×10^{-4}	-1.01×10^{-6}	9.72	-2.65×10^{-2}

Table 9. Comparison of various kinematics for the B/F/B plate: evaluation of in-plane stresses and electric and magnetic potentials; FEM results found for electric and magnetic potentials does not converge to the exact solution for the reason explained in Sec.E

	$\sigma_{33}[Pa]$ top face	$\sigma_{13}[Pa]$ center	$u_1[m]$ bottom face	$u_3[m]$ bottom face
3D[17]	0.5	-3.86×10^{-1}	-1.57×10^{-12}	4.38×10^{-12}
FEM LD1	0.83	-3.97×10^{-1}	-1.55×10^{-12}	4.33×10^{-12}
FEM LD2	0.53	-4.11×10^{-1}	-1.583×10^{-12}	4.40×10^{-12}
FEM LD3	0.51	-4.06×10^{-1}	-1.584×10^{-12}	4.40×10^{-12}
FEM LD4	0.51	-4.06×10^{-1}	-1.585×10^{-12}	4.40×10^{-12}
FEM ED1	1.56	-1.25×10^{0}	-1.30×10^{-13}	4.00×10^{-12}
FEM ED2	8.73	-3.22×10^{-1}	-1.57×10^{-13}	5.44×10^{-12}
FEM ED3	3.91	-7.84×10^{-1}	-1.58×10^{-13}	5.56×10^{-12}
FEM ED4	16.4	-1.95×10^{-1}	-1.59×10^{-13}	5.64×10^{-12}

Table 10. Comparison of various kinematics for the F/B/F plate: evaluation of transverse stresses and displacements

	$\phi_{MAX}[V]$	$\psi_{MAX}[C/s]$	$\sigma_{11}[Pa]$ top face	σ_{12}[Pa] bottom face
3D[17]	2.30×10^{-3}	-1.88×10^{-6}	1.33	-5.69×10^{-1}
FEM LD1	5.54×10^{-4}	-1.63×10^{-7}	1.6	-5.49×10^{-1}
FEM LD2	5.56×10^{-4}	-1.53×10^{-7}	1.44	-5.74×10^{-1}
FEM LD3	5.58×10^{-4}	-1.55×10^{-7}	1.42	-5.74×10^{-1}
FEM LD4	5.58×10^{-4}	-1.55×10^{-7}	1.42	-5.74×10^{-1}
FEM ED1	4.48×10^{-4}	-3.00×10^{-6}	2.65	-4.81×10^{-2}
FEM ED2	4.84×10^{-4}	-1.90×10^{-6}	8.26	-4.18×10^{-2}
FEM ED3	5.62×10^{-4}	-1.73×10^{-6}	6.89	-4.21×10^{-2}
FEM ED4	5.10×10^{-4}	-1.41×10^{-6}	15.9	-3.61×10^{-2}

Table 11. Comparison of various kinematics for the F/B/F plate: evaluation of in-plane stresses and electric and magnetic potentials; FEM results found for electric and magnetic potentials does not converge to the exact solution for the reason explained in Sec.E

VII. Conclusions

The PVD variational statement has been discussed for thermo-magneto-electro-mechanical multifield problems and for the relative subcases of coupling. Multilayered plates and the related finite elements have been considered in the framework of the Carrera's Unified Formulation. A FEM Fortran SW called MUL2 has been developed coherently with the presented formulation and several multifield results have been compared with exact solutions available in literature. It has been showed that numerical results are in good agreement with the referenced exact solutions. This paper is devoted to FEs based on PVD. In future works, the same assessments will appear also for FEs based on the Reissner's Mixed Variational Theorem, which is very suitable to obtain a fast convergence for stresses and for other non-mechanical quantities hard to calculate in multifield problems. The present formulation, together with the developed MUL2 code, represents a valuable tool to run many kind of fully coupled multifield analysis dealing with multilayered structures.

VIII. Acknowledgements

This work has been carried out with the partial support of European Space Agency, ESTEC-Contract No. 21082/06/NL/PA.

References

[1] T. Ikeda, "Fundamentals of piezoelectricity", *Oxford Science pubblications*, 1996.

[2] E. Carrera, S. Brischetto, and P. Nali, "Variational statements and computational models for multifield problems and multilayered structures", *Special Issue of MAMS, in press.*

[3] E. Carrera, "Historical review of zig-zag theories for multilayered plates and shells", *Applied Mechanics Review*, vol. 56, pp. 287–308, 2003.

[4] E. Carrera and S. Brischetto, "Piezoelectric shell theories with a priori continuous transverse electromechanical variables", *JOMMS*, vol. 2, no. 2, 2007.

[5] E. Carrera and C. Fagiano, "Mixed piezoelectric plate elements with continuous transverse electric displacements", *JOMMS*, vol. 2, no. 3, 2007.

[6] G. A. Altay and M. C. Dokmeci, "Fundamental variational equations of discontinuous thermopiezoelectric fields", *International Journal Engineering Science*, vol. 34, no. 7, pp. 769–782, 1996.

[7] E. Carrera, M. Boscolo, and A. Robaldo, "Hierarchic multilayered plate elements for coupled multifield problems of piezoelectric adaptive structures: formulation and numerical assessment", *Archives of Computational Method in Engineering, in press.*

[8] Y. Jiashi, "Electric, optic and acoustic interactions in crystals", *Whiley, New York*, p. 74, 1979.

[9] D. Nelson, "Fundamentals of piezoelectriticy", *Oxford University Press*, 1996.

[10] E. Carrera, "An assessment of mixed and classical theories for the thermal stress analysis of orthotropic multilayered plates", *Journal of Thermal Stress*, vol. 23, pp. 797–831, 2000.

[11] E. Carrera and P. Nali, "Description of a symbolic code able to calculate the unified formulation fundamental nuclei for pvd and rmvt variational statements", *DIASP internal report, Politecnico di Torino*, 2007.

[12] E. Carrera and L. DeMasi, "Classical and advanced multilayered plate elements based upon pvd and rmvt. part 2. numerical implementations", *International Journal Numerical Methods in Engineering*, vol. 55, pp. 253–291, 2002.

[13] K. Bhaskar, T. K. Varadan, and J. S. M. Ali, "Thermoelastic solutions for orthotropic and anisotropic composite laminates", *Composites*, vol. 27B, pp. 415–420, 1996.

[14] V. Tungikar and K. Rao, "Three dimensional exact solution of thermal stresses in rectangular composite laminate", *Composite structures*, vol. 27, pp. 419–430, 1994.

[15] E. Carrera and S. Brischetto, "Analysis of thickness locking in classical, refined and mixed multilayered plate theories", *Composite Structures*, vol. 82, pp. 449–562, 2008.

[16] P. Heyliger and D. Saravanos, "Exact free-vibration analysis of laminated plates with embedded piezoelectric layers", *Journal of Acoustical Society of America*, vol. 98, no. 3, pp. 1547–1557, 1995.

[17] E. Pan, "Exact solution for simply supported and multilayered magneto-electro-elastic plates", *Journal Of Applied Mechanics*, vol. 68, pp. 608–618, 2001.

[18] E. Carrera, M. D. Gifico, P. Nali, and S. Brischetto, "Refined multilayered plate elements for coupled magneto-electro-elastic analysis", *Multidisccipline Modeling in Materials and Structures*, in press.